Substrate access channel topology in membrane-bound prostacyclin synthase

Hui DENG, Aimin HUANG, Shui-Ping SO, Yue-Zhen LIN and Ke-He RUAN[1]

The Vascular Biology Research Center and Division of Hematology, Department of Internal Medicine, The University of Texas Health Science Center, Houston, TX 77030, U.S.A.

Results from our molecular-modelling and site-directed-mutagenesis studies of prostaglandin I_2 synthase (PGIS) have suggested that the large PGIS cytoplasmic domain is anchored to the endoplasmic reticulum (ER) membrane by the N-terminal segment in a way that orients the substrate access channel opening to face the membrane. To test this hypothesis we have explored the accessibility of the PGIS substrate channel opening to site-specific antibodies. The working three-dimensional PGIS model constructed by protein homology modelling was used to predict surface portions near the substrate access channel opening. Two peptides corresponding to the surface immediately near the opening [residues 66–75 (P66–75) and 95–116 (P95–116)], and two other peptides corresponding to the surface about 10–20 Å (1 Å = 0.1 nm) away from the opening [residues 366–382 (P366–382) and 472–482 (P472–482)] were used to prepare site-specific antibodies. All four antipeptide antibodies specifically recognized the synthetic segments of human PGIS and recombinant PGIS, as shown by binding assays and Western-blot analysis. The site-specific antibodies were used to probe the accessibility of the substrate access channel opening in transiently transfected COS-1 cells expressing recombinant human PGIS, and in spontaneously transformed human endothelial cell line ECV cells expressing endogenous human PGIS. Immunofluorescence staining was performed for cells selectively permeabilized with streptolysin O and for cells whose membranes were permeabilized with detergent. Antibodies to peptides in the immediate vicinity of the substrate channel (P66–75 and P95–116) bound to their targets only after general permeabilization with Triton X-100. In contrast, the two antibodies to peptides further from the channel opening (P366–382 and P472–482) bound to their targets even in cells with intact ER membranes. These observations support our topology model in which the PGIS substrate access channel opening is positioned close to the ER membrane.

Key words: cytochrome P450, membrane topology, peptide antibody, prostaglandin, prostaglandin I_2 synthase.

INTRODUCTION

Prostaglandin I_2 synthase (PGIS), a cytochrome P450, contains 500 amino acids with a calculated molecular mass of about 57 kDa [1–3] and is located in the endoplasmic-reticulum (ER) membrane [4–6]. PGIS converts prostaglandin H_2 (PGH_2) into prostaglandin I_2 (PGI_2), a potent inhibitor of platelet aggregation, vasoconstriction and leucocyte interactions with endothelium [7,8]. PGI_2 biosynthesis presumably involves efficient co-ordination in the ER membrane between PGIS and prostaglandin H_2 synthase (PGHS), which produces PGH_2. Results from crystallography and topology studies have indicated that the catalytic domain of PGHS is on the luminal side of the ER, with the cyclo-oxygenase substrate channel of PGHS immersed in the ER membrane [9–11]. The PGHS lipid substrate, arachidonic acid, thus appears to be delivered to the cyclo-oxygenase channel via the ER lipid bilayer. PGIS being a member of the microsomal P450 superfamily, its catalytic domain is believed to be anchored to the ER membrane by an N-terminal membrane anchor segment, positioning the PGIS catalytic domain facing the cytoplasmic side of the ER. Our recent peptidoliposome reconstitution and CD spectroscopy studies of the PGIS N-terminal membrane domain concluded that the PGIS N-terminal membrane anchor domain is similar to other microsomal P450s [12]. The PGIS substrate, PGH_2, is thus produced on the ER luminal side and must pass across the ER membrane barrier to reach the catalytic portion of PGIS on the cytoplasmic side. Whether the lipophilic substrate, PGH_2, presents to the synthase directly via the lipid membrane is unknown. The possible models of the substrate access opening of PGIS can be proposed in two ways: (1) facing the ER membrane to receive the hydrophobic substrate directly through the lipid membrane, or (2) exposed on the ER surface to receive the substrate from the aqueous environment (Figure 1). For other microsomal P450s, Nelson and Strobel [13] developed a model for how P450s interact with the membrane, in which the P450 is anchored to the membrane by the N-terminal hydrophobic domain and the Cys-ligand surface predicted to be the main site of interaction with redox partners is oriented away from the membrane, leaving this region available for interaction with the soluble domain of cytochrome P450 (P450) reductase. This orientation places the substrate access opening facing the membrane. Our working models developed for thromboxane A_2 synthase (TXAS) and PGIS by homology modelling strategies using $P450_{BM\text{-}3}$, a bacterial P450, as a template, which has a similar substrate-binding cavity [14–16], have indicated that the substrate openings are near the N-terminal membrane-anchor domains. These imply that the substrate access channel openings of PGIS and TXAS face the ER membrane. To test the model, in the present study we have prepared a series of antibodies against the epitopes predicted, by modelling, to be located on the PGIS surface near the opening or on the surface some distance away. These site-specific antibodies

Abbreviations used: ER, endoplasmic reticulum; PGIS, prostaglandin I_2 synthase; TXAS, thromboxane A_2 synthase; PGHS, prostaglandin H_2 (PGH_2) synthase; SLO, streptolysin O; P450, cytochrome P450; KLH, keyhole-limpet haemocyanin; PDI, protein disulphide-isomerase; 3-D, three-dimensional.

[1] To whom correspondence should be sent, at the following address: Division of Hematology, Department of Internal Medicine, University of Texas Health Science Center at Houston, 6431 Fannin St, Houston, TX 77030, U.S.A. (e-mail kruan@uth.tmc.edu).

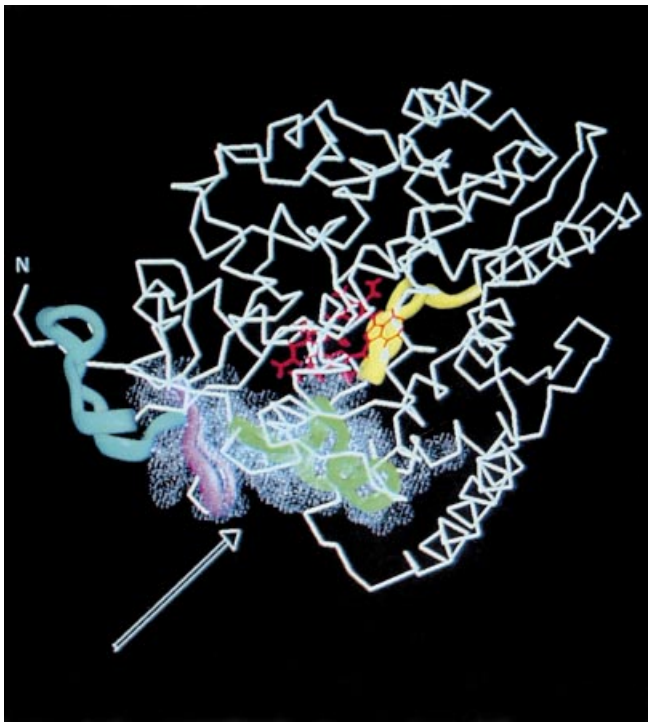

Figure 1 Constructed 3-D structural model of human PGIS based on the $P450_{BM-3}$ X-ray structure

Four segments with residues 66–75 (magenta), 95–116 (green), 366–382 (blue) and 472–482 (yellow) synthesized for site-specific antibody production are highlighted with ribbons. The red structure denotes haem; the arrow denotes channel opening.

were used to characterize the accessibility of the epitopes in permeabilized COS-1 cells expressing recombinant PGIS and in ECV (spontaneously transformed human umbilical vein endothelial cell line) cells expressing endogenous PGIS. The results indicate that the surface epitopes, away from the substrate opening, were readily accessed by the site-specific antibodies, but surface epitopes near the opening could not be accessed unless the ER membrane was disrupted. These data support a topological model in which the bulk of the PGIS protein lies on the cytosolic side of the ER bilayer, with the substrate access channel opening close to and facing the ER membrane.

EXPERIMENTAL

Molecular modelling

The strategy used for constructing the PGIS three-dimensional (3-D) model followed that developed for TXAS [14] and other mammalian P450s [17]. In brief, the strategy took consideration of six procedures: (i) sequence alignment, (ii) framework construction, (iii) loop structural determination, (iv) side-chain placement, (v) molecular docking and (vi) energy minimization [14,15]. A sequence-similarity alignment was made for human PGIS and the haemoprotein domain of $P450_{BM-3}$. The main-chain conformation of PGIS was built by transferring the crystal co-ordinates of $P450_{BM-3}$ to the aligned components of PGIS. The backbone segments were linked to each other using a fragment searching approach and a database containing 58 protein three-dimensional structures with highest resolution, developed by Ruan and colleagues [14,15].

Peptide synthesis

Peptides were synthesized by the solid-phase method using Fmoc (fluoren-9-ylmethoxycarbonyl) chemistry and cleaved with 90 % (w/v) trifluoroacetic acid [18,19]. The peptides were purified to homogeneity using HPLC on a Vydac C_4 or C_{18} reversed-phase column with a gradient of acetonitrile in aqueous trifluoroacetic acid [20,21]. The molecular masses of the purified peptides were verified by using MS [22].

Immunization and characterization of peptide antibodies

Each HPLC-purified peptide was coupled to keyhole-limpet haemocyanin (KLH) using glutaldehyde [20]. Female New Zealand White rabbits were immunized with 200 μg of peptide–KLH conjugate in Freund's complete adjuvant; booster immunizations with 200 μg of conjugate in Freund's incomplete adjuvant were given on days 14, 28 and 48. Blood was collected from the marginal ear vein starting 7 days after the final injection, and IgG fractions were isolated from the resulting antisera by Na_2SO_4 precipitation and DE52-cellulose ion-exchange chromatography [23]. The antibodies were further purified by affinity chromatography using the appropriate peptide immobilized on CNBr-activated Sepharose 4B [20,24]. Anti-(human PGIS) antibody was obtained from Dr Lee-Ho Wang, Division of Hematology, Department of Internal Medicine, The University of Texas Health Science Center at Houston, Houston, TX, U.S.A. [15].

Cell culture and transfection

Recombinant PGIS was expressed in COS-1 cells as described in [15]. Briefly, COS-1 cells were cultured at 37 °C in a humidified 5 %-CO_2 atmosphere on a coverslip with Dulbecco's modified Eagle's medium containing 10 % (v/v) fetal-calf serum to near confluence ($\approx 2.5 \times 10^6$ cells/dish). The cells were transfected with purified cDNA in the presence of DEAE-dextran and then grown for 48 h before harvesting. Alternatively, intact cells were processed for immunofluorescence staining on the coverslip intended [20]. ECV cells were grown in Medium 199 containing 10 % fetal-calf serum in a humidified 5 %-CO_2 atmosphere.

Microsome preparation and immunoblotting

The general procedures for microsome preparation and immunoblotting were carried out as described previously [20,25]. The transfected COS-1 cells or ECV cells were scraped from the plates into ice-cold 0.1 M Tris/HCl containing 0.5 mM PMSF and 10 μM indomethacin, pH 7.4, and collected by centrifugation. The pellet was resuspended in the same buffer, sonicated briefly, and centrifuged at 10000 ***g*** for 10 min. The supernatant liquid was centrifuged at 200000 ***g*** for 40 min to pellet the microsomal fraction, which was resuspended in a small volume of the same buffer. Microsomal proteins were separated by 10 %-(w/v)-PAGE under denaturing conditions and then transferred to a nitrocellulose membrane. Bands recognized by particular primary antibodies were visualized with horseradish peroxidase-conjugated secondary antibody and chromogenic peroxidase substrate [15,20].

Antibody binding assay

Binding of antibody to the corresponding synthetic peptides or the recombinant protein of human PGIS was assessed by enzyme immunoassay as described previously [20].

Indirect immunofluorescence

Procedures used for selective permeabilization of cell membranes were described previously [10,20]. Briefly, ECV cells or transfected COS-1 cells grown on coverslips were washed with 25 mM Hepes, pH 7.4, containing 2.5 mM magnesium acetate, 25 mM KCl and 250 mM sucrose (Hepes buffer) and then incubated at 0 °C (for selective permeabilization of the plasma membrane) or 37 °C (for general permeabilization of plasma and ER membranes) for 10 min with 1.6 units/ml streptolysin O (SLO), which had been pre-activated with 4 mM dithiothreitol in Hepes buffer at 37 °C for 10 min. After excess toxin was removed by washing twice with Hepes buffer at 0 °C, the cells were incubated at 37 °C for 15 min, fixed with 1% formaldehyde for 10 min, and then blocked with 1% goat serum containing 5 mg/ml glycine in Hepes buffer for 20 min. The fixed cells were then incubated with 10 μg/ml of purified IgG or antisera (1:200 dilution) in Hepes buffer containing 10% goat serum at 24 °C for 1 h. After washing three times with Hepes buffer, the cells were incubated with goat anti-rabbit IgG–FITC conjugate (1:50 dilution, Sigma) in Hepes buffer for 1 h. Washing several times with the sodium-free Hepes buffer, the cells were mounted in Mowiol 4-88 (Calbiochem) containing 2.5% triethylenediamine (Sigma) and protected by a glass coverslip. For alternate general permeabilization, the cells were incubated with 5% Triton X-100 for 20 min, then washed and incubated with the primary and secondary antibodies in the presence of 0.5% Triton X-100 as described above [20]. Cells stained with the FITC conjugate were viewed with an Olympus Model BH-2 epifluorescence microscope.

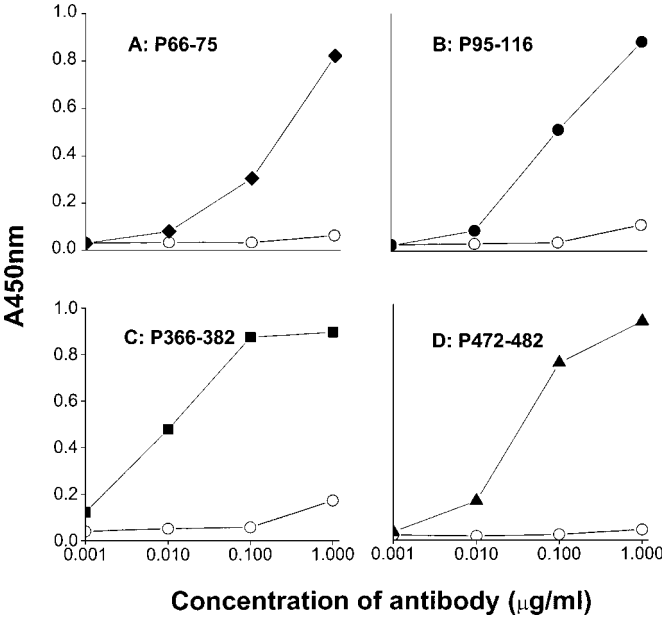

Figure 2 Binding of affinity-purified peptide antibodies to their peptide antigens

Microtitre-plate wells were coated with 50 μl of individual peptide P66–75 (**A**), 95–116 (**B**), P366–382 (**C**) or P472–482 (**D**) at 4 °C overnight and then incubated with 50 μl of the indicated concentration of the corresponding peptide antibody purified by affinity chromatography (closed symbols) or pre-immune antibody (open symbols) at 37 °C for 2 h. After washing, the bound antibody was quantified as described in the Experimental section.

RESULTS

Design of peptides to probe the accessibility of surfaces near the PGIS substrate access channel

The working 3-D model of PGIS was used to identify surface portions near the substrate access channel opening. The accessibility of the surface regions in the native ER-membrane-bound PGIS provides information about the position of the substrate channel opening relative to the membrane. Two peptides corresponding to the surface immediately near the substrate channel opening [residues 66–75 (P66–75) and 95–116 (P95–116)] and another two peptides predicted to be on the surface about 10–20 Å away from the opening [residues 366–382 (P366–382) and 472–482 (P472–482)] (Figure 1) were selected. The predicted antigenicity and exposure surface of the peptides was checked by hydropathy and secondary-structural analyses using multiple methods. All four peptide segments were predicted to be relatively hydrophilic and to adopt turn structures consistent with predictions from the 3-D working model. The four peptide segments were synthesized, purified, coupled to carrier protein and used to immunize rabbits for production of specific peptide antibodies as described in the Experimental section.

Site-specific antibody purification and characterization

Polyclonal antibodies were fractionated and purified as described in the Experimental section. The purified antibodies were tested for their ability to bind to the target peptide antigens (Figure 2). High titres of antibody binding to cognate peptide were observed for all four site-specific antibodies. In contrast, the pre-immune antibodies did not bind significantly to the target PGIS peptides (Figure 2). The unique binding specificity of the site-directed antibodies was further characterized by enzyme immunoassay using a combination test (Figure 3). The specificity of the antibodies was confirmed by the binding to their target site-specific peptides but not cross-binding to other peptides (Figure 3). Recognition of the site-specific antibodies to the native

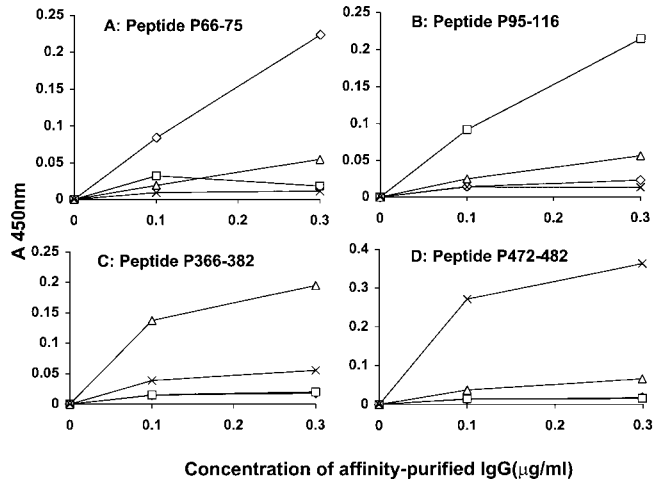

Figure 3 Binding of affinity-purified peptide antibodies with indicated concentration to the corresponding peptide antigen and other peptide antigens

The antibodies used are: antipeptide P66–75 (◇), antipeptide P95–116 (□), antipeptide P366–382 (△) and antipeptide P472–482 (×). Data were obtained as described for Figure 2.

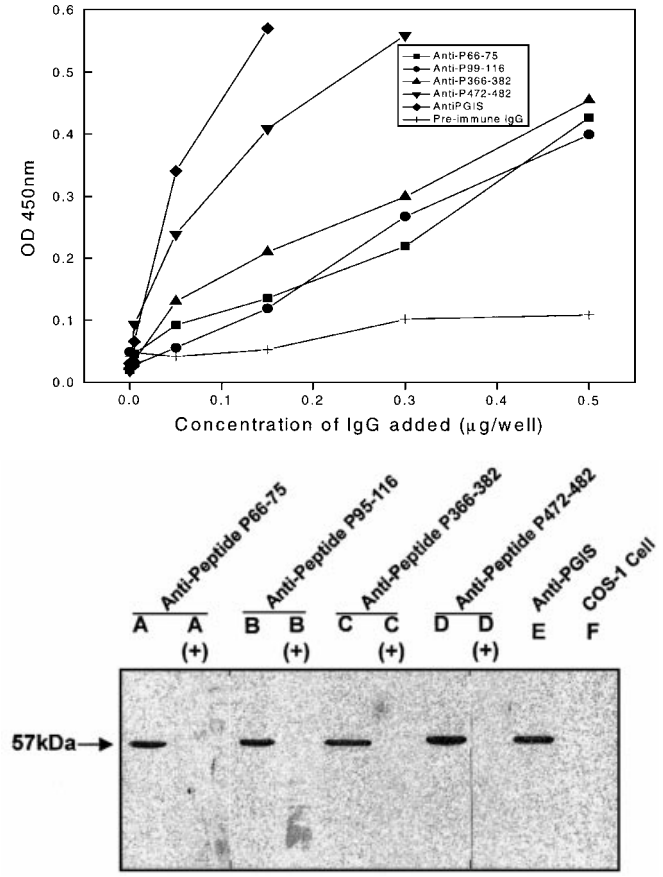

Figure 4 Binding of affinity-purified antibodies to recombinant human PGIS protein (upper panel) and Western-blotting analysis of the peptide antibodies binding to human PGIS protein (lower panel)

Upper panel: microtitre-plate wells were coated with 1 μg of octyl glucoside-solubilized recombinant PGIS protein at 4 °C overnight and then incubated with the indicated concentration of the antibodies at 37 °C for 2 h. After washing, bound antibody was quantified as described in the Experimental section. Lower panel: a 60 μg sample of transfected COS-1 cell protein, separated by SDS/10%-(w/v)-PAGE, was transferred on to a nitrocellulose membrane. The membrane was probed with individual anti-(peptide P66–75) (lane A), -(peptide P95–116) (lane B), -(peptide P366–382) (lane C) and -(peptide P472–482) (lane D) antibodies (10 μg/ml), which were untreated (lanes A, B, C or D) or pre-incubated with 1 ml of corresponding peptide–Sepharose 4B (1 mg of peptide/1 ml of Sepharose 4B) for 4 h [lanes A(+), B(+), C(+) and D(+)] or anti-(human PGIS) (lane E) antibody. Lane F is a non-transfected COS-1 cell allowed to react with anti-PGIS antibody. The positions of molecular-mass standards are not shown. The arrow shows the position of PGIS protein. OD 450 nm = A_{450}.

(Figure 4, upper panel) or denatured (Figure 4, lower panel) recombinant PGIS protein was examined by enzyme immunoassay and immunoblotting. All of the purified peptide antibodies have similar affinities bound to the native PGIS protein (Figure 4, upper panel), and recognize the denatured PGIS protein, giving a single band with an apparent molecular mass of 57 kDa (Figure 4, lower panel), as expected for the PGIS monomer [1]. The pre-immune IgG did not show significant binding to PGIS in the enzyme immunoassay and the immunoblotting (Figure 4). The specific binding on the Western blot was confirmed by the blocking of the binding using the peptide antibody pre-incubated with corresponding peptide–Sepharose 4B [Figure 4, lower panel, A(+), B(+), C(+) and D(+)]. These results demonstrated that the corresponding antibody could specifically recognize the four target segments of human PGIS.

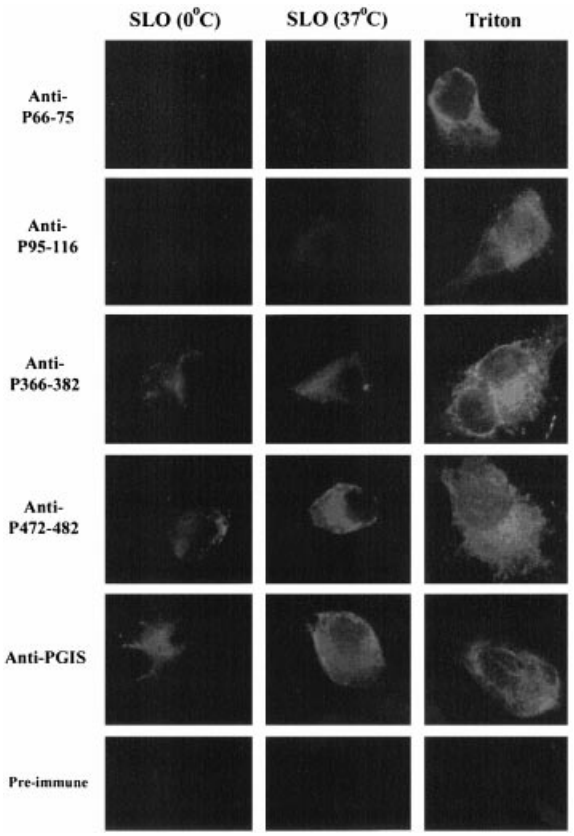

Figure 5 Immunofluorescence micrographs of COS-1 cells stained with anti-(PGIS peptide) antibodies

COS-1 cells transfected with human PGIS cDNA were permeabilized with SLO at 0 °C or SLO at 37 °C or Triton X-100. Permeabilized cells were incubated with 10 μg/ml affinity-purified peptide antibody and stained with the FITC-labelled secondary antibody. All photomicrographs were taken with the same exposure times (magnification 500 ×).

Accessibility of target peptides in recombinant PGIS exposed in COS-1 cells

The affinity-purified site-specific peptide antibodies were used as probes to examine the topology of the substrate access channel opening in transiently transfected COS-1 cells expressing recombinant human PGIS. Immunofluorescence staining was performed for cells permeabilized with SLO at 0 °C or 37 °C and for cells whose membranes were disrupted with detergent (Figure 5). SLO treatment at 0 °C was used to selectively permeabilize the plasma membrane without perturbing the ER membrane. SLO treatment at 37 °C was used to permeabilize the plasma and internal membranes and allow the antibodies to reach the luminal side of the ER membrane [10,20]. Triton X-100, a non-ionic detergent, was used to achieve maximal exposure of ER membrane proteins [20]. To confirm that the desired permeabilization was achieved, transfected COS-1 cells permeabilized with the various treatments described above were incubated with rhodamine-labelled phalloidin (targeted at actin in the cytoplasmic compartment) or with antibody to protein disulphide-isomerase (PDI), which is a major ER luminal protein [10,32]. Cells permeabilized with SLO at 0 °C were stained by rhodamine-labelled phalloidin, but were not stained by antibody to PDI. In contrast, the anti-PDI antibody was able to bind its target within the ER lumen only after treatment with SLO at 37 °C or with Triton X-100 (results not shown). These results indicate that

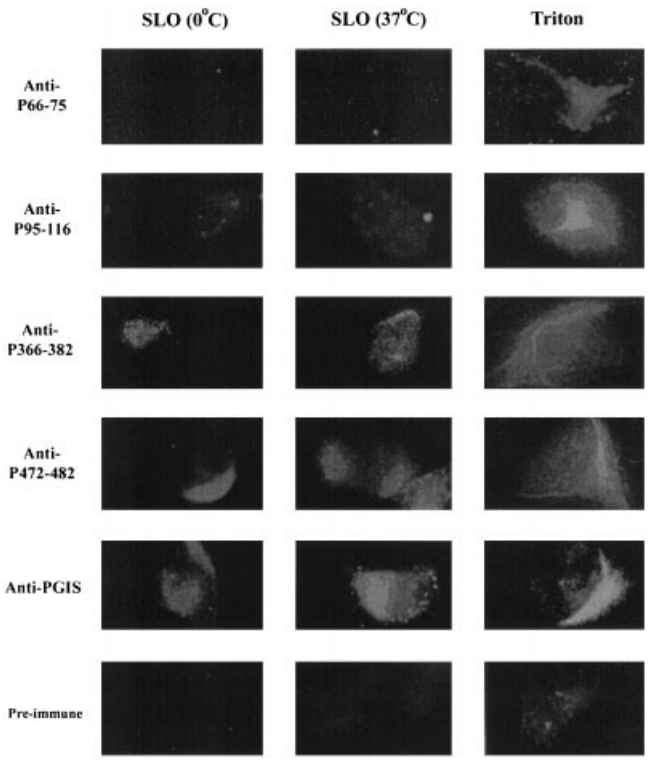

Figure 6 Immunofluorescence micrographs of ECV cells stained with anti-peptide antibodies

ECV cells were permeabilized with SLO at 0 °C or SLO at 37 °C or Triton X-100. After reaction with 10 μg/ml affinity-purified peptide antibody, the cells were stained with the FITC-labelled secondary antibody (see the Experimental section for details). Photomicrographs were obtained as described for Figure 5.

SLO treatment at 0 °C selectively breached the plasma membrane, whereas SLO treatment at 37 °C or Triton X-100 treatment disrupted both plasma and ER membranes. In addition, Triton X-100-treated cells showed diffuse staining, which reflects that the membrane was solubilized. Antibodies to PGIS peptides in the immediate vicinity of the substrate channel (P66–75 and P95–116) had access to their targets only after the membranes were disrupted with Triton X-100 (Figure 5). In contrast, the antibodies to peptides further from the channel opening (P366–382 and P472–482) had access to their targets, even when cells were treated with SLO at 0 °C, a process that leaves the ER membranes intact (Figure 5). These observations indicate that ER membrane-lipid extraction (Triton X-100 treatment) exposes the surface near the PGIS substrate channel opening, whereas toxin-mediated pore formation in the ER membrane (SLO treatment at 37 °C) leaves the substrate channel opening region blocked.

Accessibility of target peptides in endogenous PGIS in ECV cells

To confirm the immunocytochemical results obtained with recombinant PGIS expressed in COS-1 cells, similar experiments were performed on ECV cells, which have endogenous PGIS (Figure 6). ECV cells were permeabilized with SLO at 0 °C or 37 °C, or with Triton X-100, incubated with one of the four site-specific peptide antibodies and then stained with FITC-labelled second antibody as described above for the COS-1 cells. Antibodies against the peptides near the substrate channel opening (P66–75 and P95–116) had access to their targets only after the membranes were disrupted with Triton X-100 (Figure 6). The site-specific antibodies to peptides away from the channel opening (P366–382 and P472–482) had access to their targets, even when cells were treated with SLO at 0 °C, a process that leaves ER membranes intact (Figure 6). These observations indicated that the general topology of the substrate access channel opening in recombinant PGIS overexpressed in COS-1 cells is similar to that of native PGIS in ECV cells.

DISCUSSION

The working 3-D model constructed for PGIS by protein homology modelling was used to identify surface portions near the substrate access channel opening. A crystallographic structure has not been determined for any wild-type mammalian P450. However, a crystallographic structure of the haemoprotein domain of $P450_{BM-3}$, which is considered to be functionally related to microsomal P450s, has been determined at 2.0 Å resolution [26]. The structural similarity of $P450_{BM-3}$ to eicosanoid-synthesizing P450s, PGIS and TXAS is reflected in their 25 % sequence identity and the substrate similarity. PGH_2, a substrate for PGIS and TXAS, is derived from arachidonic acid, which is a substrate for $P450_{BM-3}$. The substrate-binding cavities of PGIS and TXAS may therefore have geometric arrangements similar to the substrate-binding pocket of $P450_{BM-3}$. On the basis of the crystallographic structure of the $P450_{BM-3}$, we had previously constructed a detailed 3-D structural working model of TXAS using the QUANTA-CHARMm protein-modelling package (Molecular Simulations Inc., San Diego, CA, U.S.A.) on a Silicon Graphics (Mountain View, CA, U.S.A.) workstation [14]. The accuracy of the 3-D model has partially been confirmed by site-directed mutagenesis for the several important residues predicted from the 3-D working model, which are involved in the making up of the substrate- or haem-binding sites of TXAS [16]. The observation that the crystallographic structure of $P450_{BM-3}$ serves as a suitable template for construction of the 3-D model of TXAS has supported the creation of a 3-D working model for human PGIS (Figure 1) using a protein-modelling process similar to that employed for TXAS. Overall, the conserved helical segments of the haemoprotein domain of $P450_{BM-3}$, which have provided the backbone and which have also contributed to important haem- and substrate-binding regions have suggested that the 3-D working model has provided a good approximation to the general folding figure of the substrate-binding channel. A way to evaluate further the accuracy of the general geometric folding of the substrate-binding channel is to identify the key residues that are important in making up the channel, predicted from the working model. Cys^{441} and several other residues which are assigned as part of the haem-interaction or substrate-binding pocket from the model have been mutated and confirmed to be important for enzyme activity [15]. These findings have let us use the 3-D working model of human PGIS for the prediction of the opening surface of the substrate-binding channel.

In order to exclude the possibility that the Triton X-100 detergent solubilization may expose an internally buried site to change the protein folding, we have performed a Triton X-100 or octyl glucoside-solubilized PGIS activity assay, in which the synthase activity was not significantly affected by the non-ionic detergents (results not shown). This result supports the fact that detergent-solubilized synthase did not change major protein folding. The immunofluorescent staining for the Triton X-100-treated cells is able to determine the native form of PGIS distributed on the ER membrane.

The peptide antibody staining described in the Results section provides direct experimental evidence to support the model in which the substrate channel opening of PGIS is facing and in contact with the ER membrane. Then the PGIS substrate access surface would be opened and exposed to the lipid bilayer, raising the possibility that the bilayer itself forms part of the access channel. The PGIS lipophilic substrate, PGH_2, derived from arachidonic acid by PGHS, would then have ready access to the PGIS active site without even leaving the membrane to contact the polar medium. This is consistent with the results from the studies of the relationship between the ER membrane and the substrate access channel for other P450s using hydrophobic drugs [27,28], and fluorescence energy transfer [29]. Alternative hypotheses can be envisaged, including the possibility of protein–protein interaction. However, it seems unlikely that PGIS interacts with other protein on the epitopes, because the upstream enzyme for PGIS, prostaglandin H2 synthase (PGHS), is located inside the ER membrane (PGIS is located outside the ER membrane) and, unlike other P450 enzymes, PGIS does not require reductase. In addition, it is unlikely that any other protein could cover two independent epitopes of PGIS at one orientation.

Crystallographic studies of detergent-solubilized [9] PGHS-1 and PGHS-2 and topological studies for membrane-bound [10,11] PGHS-1 and -2 suggest that the catalytic domains of the proteins lie on the luminal side of the ER, anchored to the membrane by hydrophobic side chains of amphipathic helices A–D. These hydrophobic side chains of the putative membrane-anchor domains also form an entrance to the substrate-binding channel and potentially form an initial docking site for the lipid substrate, arachidonic acid [9,30]. The topology models developed for PGIS described above have their catalytic domains on the cytoplasmic side of the ER, opposite to the orientation of PGHS, and both of the substrate channels of PGIS and PGHS open to the ER membrane. These suggest that the co-ordination between PGHS and PGIS in biosynthesis of PGI_2 is facilitated by the enzyme's anchoring in the lipid membrane. This predicts that the efficiency of eicosanoid biosynthesis will be different in the soluble and the membrane-bound enzymes. One indication of such a difference has been reported by Eling et al. [31], who found channeling of arachidonic acid through PGG_2 to PGH_2 in microsomal PGHS, but not in detergent-solubilized PGHS. Another observation, which supports the hypothesis, is that PGHS side-products are much less plentiful in biosynthesis of thromboxane A_2 and PGI_2 with intact membrane-bound systems as compared with solubilized enzymes. This suggests that the lipid substrates, arachidonic acid and PGH_2 have higher-efficiency access to the active sites and less chance to be degraded in the membrane-bound systems.

Characterization of the substrate access channel opening for PGIS described in the present paper also provides general topological information for the important regions of other eicosanoid-synthesizing P450 enzymes, such as TXAS, which shares the same substrate with PGIS. However, TXAS converts PGH_2 into thromboxane A_2 which is a potent platelet aggregatory and vasoconstrictive mediator with biological functions opposite to those of PGI_2. Thus the co-ordination of PGHS with TXAS in the biosynthesis of thromboxane A_2 may be different to the co-ordination with PGIS. Our previous topological studies have indicated that the large cytoplasmic domain of PGIS is anchored to the ER membrane by a single N-terminal membrane-anchor segment similar to that in other microsomal P450s, but it is quite different from TXAS, which appears to have a longer membrane-anchor segment. It is highly possible that the different N-terminal membrane-anchor format may affect the topological arrangement of the substrate access channel opening for TXAS, which may also be important to the substrate-specific recognition/docking in the co-ordination of PGHS with PGIS or TXAS. Further determination of the topology of the substrate access channel opening for TXAS in native cells will help to address this issue. In addition, the inhibition of binding of substrate-access-site antibodies to a soluble fraction of recombinant PGIS lacking the N-terminal and other possible membrane-anchoring domains would further reinforce the conclusions drawn.

We thank Dr Lee-Ho Wang for providing the PGIS cDNA, and Dr Richard J. Kulmacz and Dr Kenneth K. Wu for valuable discussions while these studies were in progress. This work was supported by National Institute of Health grants (HL56712 and NS 23327).

REFERENCES

1 Pereira, B., Wu, K. K. and Wang, L.-H. (1994) Molecular cloning and characterization of bovine prostacyclin synthase. Biochem. Biophys. Res. Commun. **203**, 59–66
2 Hara, S., Miyata, A., Yokoyama, C., Inoue, H., Brugger, R., Lottspeich, F., Ullrich, V. and Tanabe, T. (1994) Isolation and molecular cloning of prostacyclin synthase from bovine endothelial cells. J. Biol. Chem. **269**, 19897–19930
3 Miyata, A., Hara, S., Yokoyama, C., Inoue, H., Ullrich, V. and Tanabe, T. (1994) Molecular cloning and expression of human prostacyclin synthase. Biochem. Biophys. Res. Commun. **200**, 1728–1734
4 DeWitt, D. and Smith, W. L. (1983) Purification of prostacyclin synthase from bovine aorta by immunoaffinity chromatography. Evidence that the enzyme is a hemoprotein. J. Biol. Chem. **258**, 3285–3293
5 Ullrich, V., Castle, L. and Weber, P. (1981) Spectral evidence for the cytochrome p450 nature of prostacyclin synthetase. Biochem. Pharmacol. **30**, 2033–2036
6 Ullrich, V. and Graf, H. (1984) Prostacyclin and thromboxane synthase as P-450 enzymes. Trends Pharmacol. Sci. **5**, 352–355
7 Moncada, S. and Vane, J. R. (1978) Pharmacology and endogenous roles of prostaglandin endoperoxides, thromboxane A2, and prostacyclin. Pharmacol. Rev. **30**, 293–331
8 Wu, K. K. and Thiagarajan, P. (1996) Role of endothelium in thrombosis and hemostasis. Annu. Rev. Med. **47**, 315–331
9 Pico, D., Loll, P. J. and Garavito, R. (1994) X-ray crystal structure of the membrane protein prostaglandin H_2 synthase. Nature (London) **367**, 243–249
10 Ren, Y., Walker, C., Loose-Mitchell, D. S., Deng, J., Ruan, K.-H. and Kulmacz, R. J. (1995) Topology of prostaglandin H synthase-1 in the endoplasmic reticulum membrane. Arch. Biochem. Biophys. **323**, 205–214
11 Otto, J. C. and Smith, W. L. (1994) The orientation of prostaglandin endoperoxide synthases-1 and -2 in the endoplasmic reticulum. J. Biol. Chem. **269**, 19868–19875
12 Lin, Y., Wu, K. K. and Ruan, K.-H. (1998) Characterization of secondary structure and membrane interaction of the putative membrane anchor domains of prostaglandin I_2 synthase and cytochrome P450 2C1. Arch. Biochem. Biophys. **352**, 78–84
13 Nelson, D. R. and Strobel, H. W. (1988) On the membrane topology of vertebrate cytochrome P450 proteins. J. Biol. Chem. **263**, 6038–6050
14 Ruan, K.-H., Milfeld, K., Kulmacz, R. J. and Wu, K. K. (1994) Comparison of the construction of a 3-D model for human thromboxane synthase using P450 cam and BM-3 as templates: implications for the substrate binding pocket. Protein Eng. **7**, 1345–1351
15 Shyue, S.-K., Ruan, K.-H., Wang, L.-H. and Wu, K. K. (1997) Prostacyclin synthase active sites. Identification by molecular modelling-guided site-directed mutagenesis. J. Biol. Chem. **272**, 3657–3662
16 Wang, L.-H., Matijevic-Aleksic, N., Hsu, P.-Y., Ruan, K.-H., Wu, K. K. and Kulmacz, R. J. (1996) Identification of thromboxane A_2 synthase active site residues by molecular modelling-guided site-directed mutagenesis. J. Biol. Chem. **271**, 19970–19975
17 Zvelebil, M. J., Wolf, C. R. and Sternberg, M. J. E. (1991) A predicted three-dimensional structure of human cytochrome P450. Protein Eng. **4**, 271–282
18 Ruan, K.-H., Stiles, B. G. and Atassi, M. Z. (1991) Full profile of the short neurotoxin-binding regions on the extracellular part of the α-chain of human acetylcholine receptor. Biochem. J. **274**, 849–854
19 Merrifield, R. B. (1963) Solid phase peptide synthesis. The synthesis of a tetrapeptide. J. Am. Chem. Soc. **85**, 2149–2154
20 Ruan, K.-H., Wang, L.-H., Wu, K. K. and Kulmacz, R. J. (1993) Amino-terminal topology of thromboxane synthase in the endoplasmic reticulum. J. Biol. Chem. **268**, 19483–19490

21 Ruan, K.-H., Li, P., Kulmacz, R. J. and Wu, K. K. (1994) Characterization of the structure and membrane interaction of NH_2-terminal domain of thromboxane A_2 synthase. J. Biol. Chem. **269**, 20938–20942
22 Moore, W. T. and Caprioli, R. M. (1991) Monitoring peptide synthesis stepwise by mass spectrometry. In Techniques in Protein Chemistry II (Villafranca, J. J., ed.), pp. 511–528, Academic Press, New York
23 Ishikawa, E., Imagawa, M., Hashida, S., Yoshitake, S., Hamaguch, Y. and Ueno, T. (1983) Enzyme-labeling of antibodies and their fragments for enzyme immunoassay and immunohistochemical staining. Immunology **4**, 209–327
24 Ruan, K.-H., Hashida, S., Yoshitake, S., Ishikawa, E., Wakisaka, O., Yamamoto, Y., Ichioka, T. and Nakajima, K. (1985) A micro-scale affinity-purification of Fab′-horseradish peroxidase conjugates and its use for sandwich enzyme immunoassay of insulin in human serum. Clin. Chim. Acta **147**, 167–172
25 Kulmacz, R. J. and Wu, K. K. (1989) Topographic studies of microsomal and pure prostaglandin H synthase. Arch. Biochem. Biophys. **268**, 502–515
26 Ravichandran, K. G., Boddupalli, S. S., Hasermann, C. A., Peterson, J. A. and Deisenhofer, J. (1993) Crystal structure of hemoprotein domain of P450BM-3, a prototype for microsomal P450's. Science **261**, 731–736
27 Al-Gailany, K. A., Houston, J. B. and Bridges, J. W. (1978) The role of substrate lipophilicity in determining type 1 microsomal P450 binding characteristics. Biochem. Pharmacol. **27**, 783–788
28 Parry, G., Palmer, D. N. and Williams, D. J. (1976) Ligand partitioning into membranes: its significance in determining K_m and K_s values for cytochrome P-450 and other membrane bound receptors and enzymes. FEBS Lett. **67**, 123–129
29 Centeno, F. and Guiterrez-Merino, C. (1992) Location of functional centers in the microsomal cytochrome P450 system. Biochemistry **31**, 8473–8481
30 Kurumbail, R. G., Stevens, A. M., Gierse, J. K., McDonald, J. J., Stegeman, R. A., Pak, J. Y., Gildehaus, D., Miyashiro, J. M., Penning, T. D., Seibert, K. et al. (1996) Structural basis for selective inhibition of cyclooxygenase-2 by anti-inflammatory agents. Nature (London) **384**, 644–648
31 Eling, T. E., Glasgow, W. C., Curtis, J. F., Hubbard, W. C. and Handler, J. A. (1991) Studies on the reduction of endogenously generated prostaglandin G2 by prostaglandin H synthase. J. Biol. Chem. **266**, 12348–12355
32 Lin, Y.-Z., Deng, H. and Ruan, K.-H. (2000) Topology of catalytic portion of prostaglandin I_2 synthase: identification by molecular modelling-guided site-specific antibodies. Arch. Biochem. Biophys. **379**, 188–197

Received 29 April 2001/14 November 2001; accepted 13 December 2001